ISSN NO. 2320-5407

Journal homepage: http://www.journalijar.com

INTERNATIONAL JOURNAL OF ADVANCED RESEARCH

RESEARCH ARTICLE

Seasonal Statistical Study by Using Limited Area Model in Simulation of the Blocking Phenomena in Atmosphere

***A. M. Shaffie[1] & Samy A. Khalil[2]**

1. Egyptian Meteorological Authority (EMA), P.O. Box: 11784, Cairo, Egypt. Head of department of Physics, Faculty of Science & Art, Qelwah, Al - Baha University, Kingdom Of Saudi Arabia)
2. National Research Institute of Astronomy and Geophysics, Solar and Space Department, Marsed Street, Helwan, 11421 Cairo, Egypt. Department of Physics, Faculty of Science & Art, Qelwah, Al - Baha University, Kingdom Of Saudi Arabia).

Manuscript Info

Manuscript History:

Received: 10 December 2013
Final Accepted: 29 January 2014
Published Online: March 2014

Key words: Limited Area Model, Simulation, Blocking Systems, Atmosphere and Resolutions.

Corresponding Author

A. M. Shaffie

Abstract

The present thesis investigates the simulation of blocking systems by limited area model, Regional Climatic Model, (RegCM3). 6-hour datasets of geopotential height, synoptic charts and NCEP/NECAR reanalyzed at surface and 500 hpa levels through the period (1994 –2005) had been used in the present work. In addition to that the input data required for limited area model (RegCM3) has been used through that period. In winter season, the absolute error varies from 0.4 to 2.2% between the actual and estimated pressure in the first and second low, while varies from 0.5 to 12.4 in first high and second high. While in spring season the absolute error varies from (0.8 to 4.7) % between the actual and estimated pressure in the first and second low, while slightly varies between the first and second high. This due to the not differences in the pressure for actual and estimated values in first and second high is greater than in the first and second low. But in summer season the absolute error varies from (0.2 to 1.6) % between the actual and estimated pressure in the first and second low, while varies from (0.2 to 2.8) % between the first and second high, and in autumn season the absolute error varies from (0.7 to 2.9) % between the actual and estimated pressure in the first and second low, while slightly varies between the first and second high. From the above results and compared between the actual and estimated charts by using $RgCM_3$ horizontal resolution 100km, we can order the different seasonal according to the accuracy: spring, winter, autumn and summer seasons. This means that, the simulation of blocking systems using of limited area model (RegCM3) will clarify the role played by blocking systems in abnormal weather and eliminate the hazards of the sever abnormal weather phenomena which related to blocking systems.

Introduction

In fact the blocking systems consider standing long waves from Rossby waves, which characteristic by constant weather from one to four weeks, which the westerlies flow in North Hemisphere as a long waves patterns of ridges (clockwise wind) and troughs (anti-clockwise wind) as shown in figure (1). These long waves are called Rossby waves, which known as planetary waves as they owe their origin to the shape and rotation of the earth, are one of the most intriguing natural phenomena, it in the atmosphere are easy to observe as (usually 4-6) large-scale meanders of the jet stream. When these loops become very pronounced, they are detach of the masses of cold or warm air, that become cyclones and anticyclones are responsible for day-to-day weather patterns at mid-latitudes. Rossby waves

characterize the tropospheric westerlies above 500-mb level, that is, above the altitude where the pressure drops to 500-mb. Blow this level the waves are distorted some white by friction and topographic irregularities of the Earth's surface. It's more vigorous in winter than in summer because in winter the temperature contrast is greater between north and south at that time of the year, but in summer the north south temperature differences are less, the pressure gradients become weaker and as a consequence this features also ably to the westerlies (Holton, 2004).
The speed of Rossby waves is given by equation (1),

$$C = u - \beta/k^2 \qquad (1)$$

Where c is the wave speed, u is the mean westerly flow, β is the Rossby parameter, and k is the total wave number. The "weaving westerlies" have two components of motion a North–South components superimposed on the West–East components. The North–South air flow is referred to by the westerlies meridional component, while the West–East air is referred to as the zonal component. Occasionally, the westerlies flow is almost directly from West to East, nearly parallel to latitude circles, with weak meridional component as shown in figure (2).This is the zonal flow pattern in which the North–South exchange of air masses is minimal. The cold air masses remain in the North while the warm air masses remain in South. In other cases, the westerlies exhibit considerable amplitude, flowing in a pattern of deep troughs and sharp ridges as shown in figure (3).

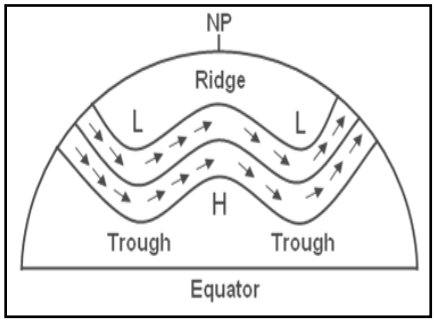

Fig (1): The Westerlies Flow in Waves Like Pattern of Ridges and Troughs

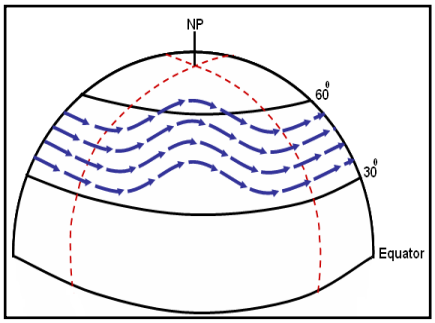

Fig (2): Middle Latitude Westerlies Exhibit a Zonal Flow Pattern

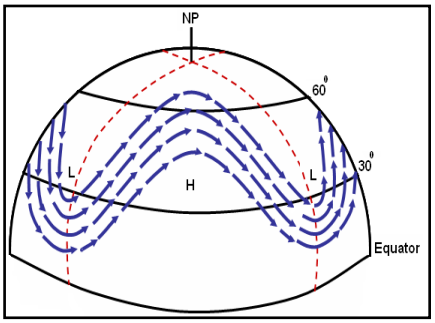

Fig (3): Middle Latitude Westerlies Exhibit a Meridional Flow Pattern

During the meridional flow pattern, masses of cold air surge southward while warm masses surge northward. Thus contrasting air masses collide, warm air overrides cold air and the stage is set for the development of storms that are then swept along by the westsrlies.

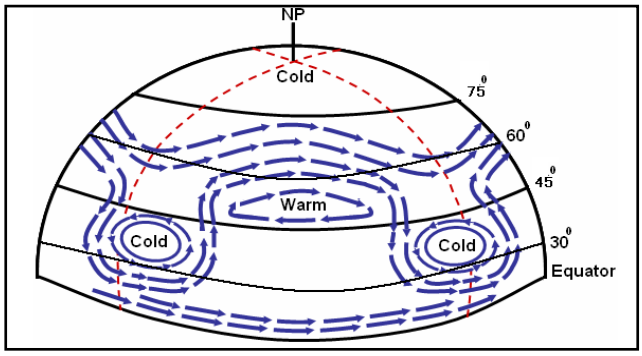

Fig (4): The Example of Omega Block

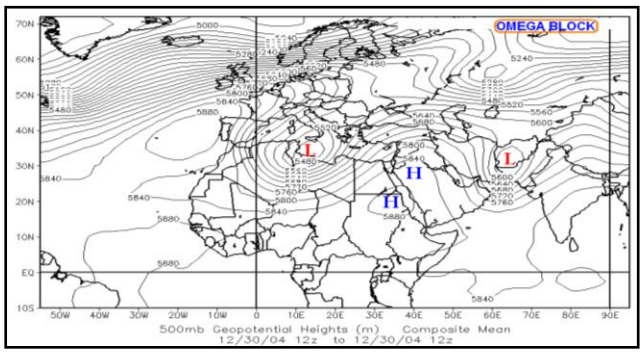

Fig (5): Actual Chart Represents Omega Shaped Block

This situation may be further complicated by a split flow pattern, in which westerlies to the North have a wave configuration that differs from that of the westerlies to the South. The westerly wind pattern typically shifts back and forth between dominantly meridional flows. The zonal flow might persist for a week and then gives way to a more meridional flow that lasts for a few weeks and then it becomes zonal flow again. The transition from one wave pattern to another is usually abrupt, sometimes taking place within a day.

Unfortunately for the long range weather forecast, the shifts between westerly wave patterns have no regularity. The only observation useful to forecasters is that meridional patterns tend to persist for longer periods then zonal flow. Blocks in meteorology are large scale patterns in the atmospheric pressure field that are nearly stationary, effectively "blocking" or redirecting migratory cyclones. They are also known as blocking highs or blocking

anticyclones. These blocks can remain in place for several days or even weeks, causing the areas affected by them to have the same kind of weather for extended period of time, (e. g. precipitation for some areas, clear skies for others).

The westerlies may become so extensive those huge whirling masses of air actually separate from the main westerlies air flow, this situation, shown schematically as shown in figure (4) and from actual chart as in figure (5). Omega blocks are so-named because the height fields associated with them resemble the Greek letter omega. The typical pattern for this is low - high - low, arranged in the west-east direction, when the pool of cold air rotating counter clock-wise is a blocking cyclone, while the pool of warm air rotating clockwise is a blocking anticyclone. The atmospheric flow pattern is occasionally dominated by quasi-persistent features whose time scale is larger than the life cycle of individual storms, but shorter than the length of a season. Such large –scale persistent feature are generally referred to as blocking.

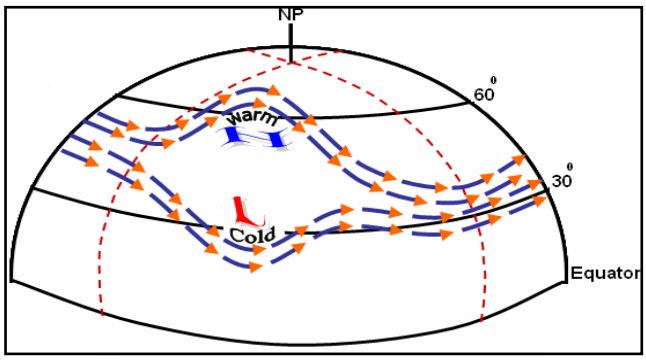

Fig (6): The Example of Diffluent Block

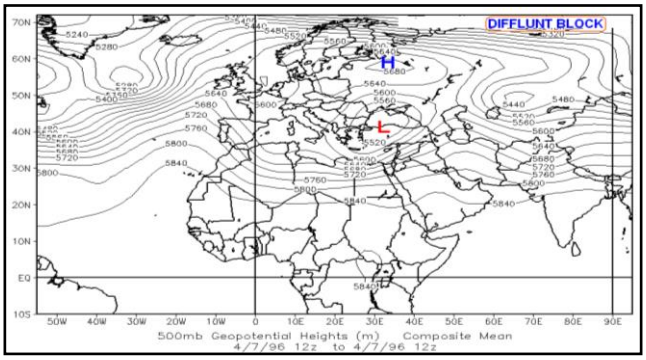

Fig (7): Actual Chart Represents Diffluent Shaped Block

In addition to "Omega" block, there are two main synoptic types which for convenience may be called "Diffluent" and "Meridional" blocks, respectively. The first type, which is also the commonest, and the jet stream separates into two distinct streams, one goes to the north east around large ware anticyclone (usually known as the blocking high) while the other circumnavigates the cold low to the south as in figure (6) and from actual chart as in figure (7).

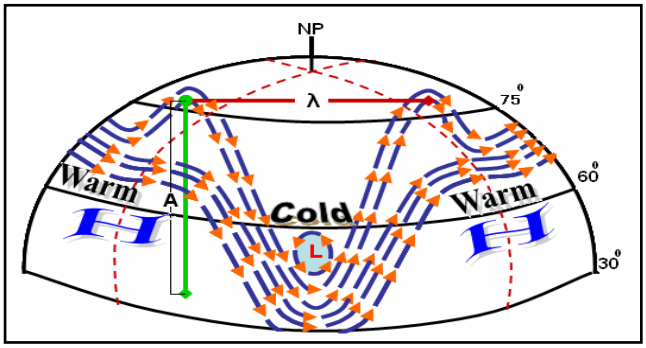

Fig (8): The Example of Meridional Block

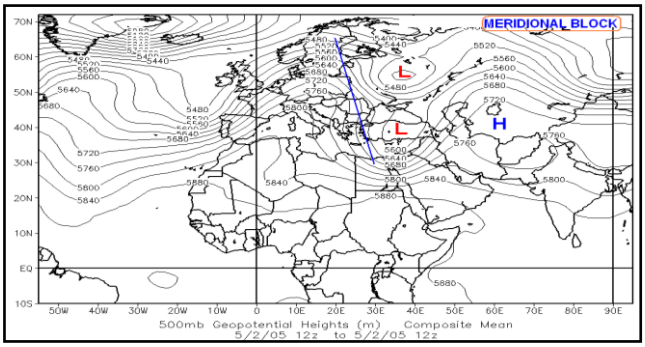

Fig (9): Actual Chart Represents Meridional Shaped Block

The second type is essentially a single upper wave of very large amplitude, which the wave length is nearly equal the amplitude in this case as in figure (8) and from actual chart as in figure (9). The anticyclonic circulation associated with it extending throughout the whole troposphere and beyond, as it does in type one. Change from one type to other frequently occurs within some of the blockings.

Blocking information by mathematical methods

If we consider the main flow of block could be steady, and the radius of weserlies is (R) and occur splitting of it as shown in figure (10). Therefore the horizontal acceleration is considered zero,(dV/dt = 0), where V is the actual wind speed. The momentum equation of motion becomes

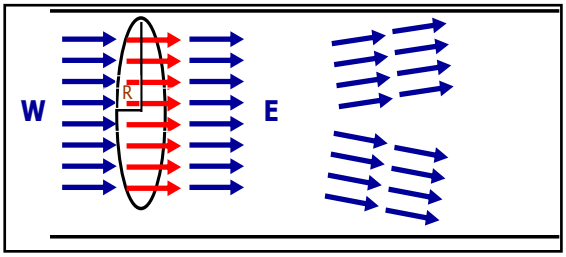

Fig (10): The Westerlies of Radius R Which Split During Move from West to East

$$0 = f\,VG + (1/\rho)(\partial p/\partial n) - (VG)2/R \qquad (2)$$

The solution of equation (2) is in the form

$$VG = +fR/2 - \sqrt{(fR/2)^2} + (R/\rho)(\partial p/\partial n) \qquad (3)$$

$$VG = -fR/2 + \sqrt{(fR/2)^2} - (R/\rho)(\partial p/\partial n) \qquad (4)$$

Where VG is the gradient wind speed, R is the radius of curvature, ρ is density, and $(\partial p/\partial n)$ is the pressure gradient. The solution of equation (3) could be used to express the air motion within the part of anticyclonic flow of the Rossby wave. Meanwhile equation (4) represents the cyclonic part of the Rossby wave. Rossby waves could be regarded as composed of cyclonic and anticyclonic flow together. For a cyclonic flow there is no restriction for an increased value of gradient wind, because pressure gradient could attain large values without any theoretical restriction. Meanwhile, for anticyclonic flow the situation is completely different. There is a critical maximum limit of gradient wind in the westerly air current. The maximum gradient wind occurs when the terms under the square root in equation (3) become zero.

$$\text{i. e.} \quad VG\ max = fR/2 \quad \text{when} \quad (fR/2)^2 = -(R/\rho)(\partial p/\partial n) \qquad (5)$$

Substituting for geostrophic wind Vg in equation (5) then, we get

$$VG\ max = 2\,Vg \qquad (6)$$

When the main westerly air current become fast enough. So that the values of gradient wind of cyclonic flow become more, the maximum gradient winds of anticyclonic flow. In such a condition the anticyclonic flow can't sustain wind speed more than its maximum gradient speed (VG max), as a result the main westerly air current splits into two branches leading to the formation of a episode. It is evident that the splitting of the main westerly air current gives only acceptable solution to prevent the appearance of imaginary term in the solution of gradient wind equation. In an anticyclonic flow the following criteria could be considered:

$$H = (fR/2)^2 + (R/\rho)(\partial p/\partial n) \qquad (7)$$

If, H, is less than zero, the solution of following equation (7) will be imaginary solution.

$$VG = -fR/2 - \sqrt{H} \qquad (8)$$

The main air current can't cross the point of negative H. Therefore, it is split into two branches (cyclonic, and anticyclonic). This is only physical solution for the equation (3), i.e. the area which have values of $H < 0$ is the area of blocking development. Moreover, the splitting persists until the value of H becomes positive. When H is positive at a grid point, then the main westerly air current crosses this point without splitting (H.M. Hasanean and Y.Y. Hafez, 2003 and Y. Y. Hafez 2012).

The Area Concerned

In order to putting the area concerned to study the blocking by using models, must be known about previous studies which describe the places of blocks, which formed from the splitting in motion of westerlies according to Rex, and in the Atlantic to the west of the Alps, and over land to the west of the Ural mountains, coincide with the maxima of the low frequency and total variance, also from the seasonal variability of persistent characteristics of waves for 500 hpa geopotential height between (20N - 70N). The aim of this paper we used this area to study the better control of resolution of grad points of a model in simulation with blocking cases in deferent seasons which effect directly on the track of cyclonic motions which across the Mediterranean and also on the motion of the annual track of the Sudan Monsoon Low which causes on weak forecast in weather in this area. It is concerned between longitudinal from (55^0W–75^0E) and latitudinal (20^0N –70^0N) as in figure (11).

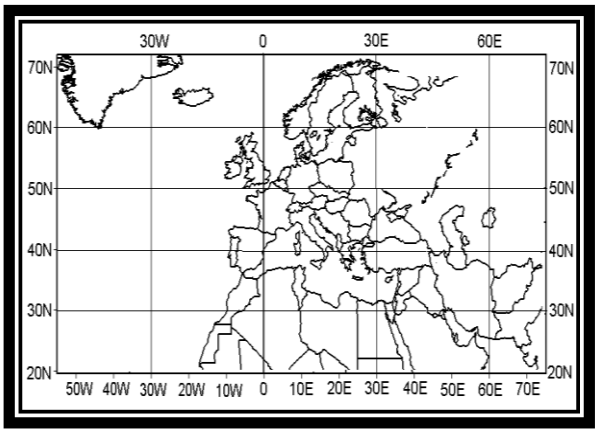

Fig (11): The Area Used in the Present Study

Limited Area Model

In fact the limited area model could be used for regional studies was originally proposed by (Dickinson et al., 1990). This idea was based on the concept of one-way nesting, in which large scale meteorological fields from General Circulation Model (GCM) runs provide initial and time-dependent meteorological lateral boundary conditions (LBCs) for high resolution Regional Climate Model (RCM) simulations, with no feedback from the RCM to the driving GCM. The first generation NCAR RegCM was built upon the NCAR-Pennsylvania State University (PSU) Mesoscale Model version 4 (MM4) in the late (1980)s (Dickinson et.al.,1989; Giorgi, 1989).

The dynamical component of the model originated from the MM4, which is compressible, finite difference model with hydrostatic balance and vertical σ- coordinates. Later, the use of a split-explicit time integration scheme (Giorgi et al., 1993a,b). As a result, the dynamical core of the RegCM is similar to that of the hydrostatic version of Mesoscale Model version 5 (MM5) (Grll et.al., 1994).

For application of the MM4 to climate studies of physics parameterization were replaced, mostly in the areas of radiative transfer and land surface physics, which led to the first generation RegCM (Dickinson et.al., 1989, Giorgi, 1990). The first generation RegCM included the Biosphere-Atmosphere Transfer Scheme, BATS, (Dickinson et al., 1986) for surface process representation, the radiative transfer scheme of the Community Climate Model version 1 (CCM1), a medium resolution local planetary boundary layer scheme, the Kuo-type cumulus convection scheme of (Anthes,1977) and the explicit moisture scheme of (Hsie et al., 1984).

A first major upgrade of the model physics and numerical schemes was documented by (Giorgi et al., 1993a,b), and resulted in second generation RegCM, hereafter referred to as REGional Climate Model version 2 (RegCM2). The physics of RegCM2 was based on that of the National Center of Atmospheric Research (NCAR) Community Climate Model version 2 (CCM2) (Hack et.al., 1993) and the mesoscale model MM5 (Grell et al., 1994). In particular, the CCM2 radiative transfer package (Briegleb, 1992) was used radiation calculations, the nonlocal boundary layer scheme of (Holtslag et.al., 1990) replaced the older local scheme, the mass flux cumulus cloud scheme of (Grell, 1993) was added as an option, and the latest version of BATSIE (Dickinson et.al., 1993) was included in the model.

In the last few years, some new physics schemes have become available for use in the RegCM, mostly based on physics schemes of the last version of the Community Climate Model (CCM), Community Climate Model version 3 (CCM3) (Kiehl et.al., 1996).

First, the CCM2 radiative transfer package has been replaced by that of the CCM3. In the CCM2 package, the effects of H2O, O3, O2, CO2 and clouds were accounted for by the model. Solar radiative transfer was treated with a δ-Eddington approach and cloud radiation depended on three cloud parameters, the cloud fractional cover, the cloud liquid water content, and the cloud effective droplet radius. The CCM3 scheme retains the same structure as that of the CCM2, but it includes new features such as effect of additional greenhouse gasses (NO2, CH4, CFCs), atmospheric aerosols, and cloud ice.

The other primary changes are in the areas of cloud and precipitation processes. The original explicit moisture scheme of (Hsie et al., 1984) has been substituted with a simplified version because the original scheme was computationally too expensive to be run in climate model. In the simplified scheme only a prognostic equation for cloud water is included, which accounts for cloud water formation, advection and mixing by turbulence, re-evaporation in sub-saturated conditions, and conversion into rain via a bulk auto conversion term. The main novelty of this scheme dose not resides of course in the simplistic microphysics, but in fact that the prognosed cloud water variable is directly used in the cloud radiation calculations. In the previous version of the model, cloud water variables for radiation calculations were diagnosed in terms of the local relative humidity.

This new feature adds a very important and far reaching element of interaction between the simulated hydrologic cycle and energy budget calculations.

Changes in the model physics include a large-scale cloud and precipitation scheme which accounts for the subgrid-scale variability of cloud (Pal et al., 2000 and Feudale I. and Shukla J., 2010), new parameterizations for ocean surface fluxes (Zeng et.al., 1998), and a cumulus convection scheme (Emanuel, 1991; Emanuel and Zivkovic-Rothman, 1999). Also new in the model is a mosaic-type parameterization of subgrid-scale heterogeneity in topography and land use (Giorgi et al., 2003b). Other improvements in RegCM3 involve the input data. The USGS Global Land Cover Characterization and Global 30 Arc-Second Elevation datasets are now used to create the terrain files. In addition, NCEP and ECMWF global reanalysis datasets are used for the initial and boundary conditions.

Lastly, improvements in the user-friendliness of the model have been made. New scripts have been included which make running the programs easier. Also, a new website has been developed where users can freely download the entire RegCM system, as well as all of the input data necessary for simulation.

The RegCM modeling system has four components: Terrain, ICBC, RegCM, and Postprocessor. Terrain and ICBC are two components of RegCM preprocessor. Terrestrial variables (including elevation, landuse and sea

surface temperature) and three-dimensional isobaric meteorological data are horizontally interpolated from a latitude-longitude mesh to a high-resolution domain on either a Rotated for (or Normal) Mercator, Lambert Conformal, or Polar Stereographic projection. Vertical interpolation from pressure levels to the σ coordinate system of RegCM is also performed. σ Surface near the ground closely follow the terrain, and the higher-level σ surface tend to approximate isobaric surfaces. Since the vertical and horizontal resolution and domain size can very, the modeling package programs employ parameterized dimensions requiring a variable amount of core memory, and the requisite hard-disk storage amount is varied accordingly.

The RegCM Model Horizontal and Vertical Grid

It is useful to first introduce the model's grid configuration. The modeling system usually gets and analyzes its data on pressure surfaces, but these have to the model's vertical coordinate before input to the model. The vertical coordinate is terrain-following Figure (12) meaning that lower grid levels follow the terrain while the upper surface is flatter. Intermediate levels progressively flatten as the pressure decreases toward the top of the model. A dimensionless σ coordinate is used define the model level where P is the pressure, Pt is a specified constant top pressure, Ps is a surface pressure.

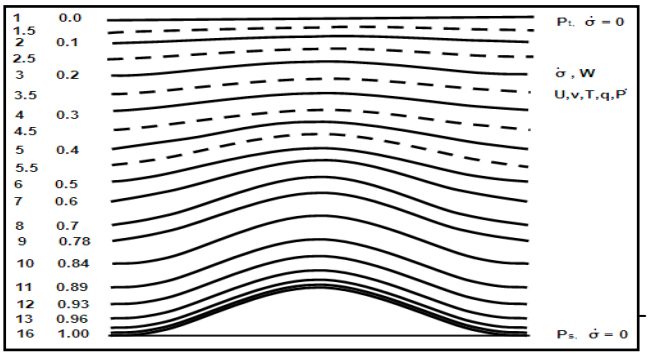

Fig (12): Schematic representation of the vertical structure of the model

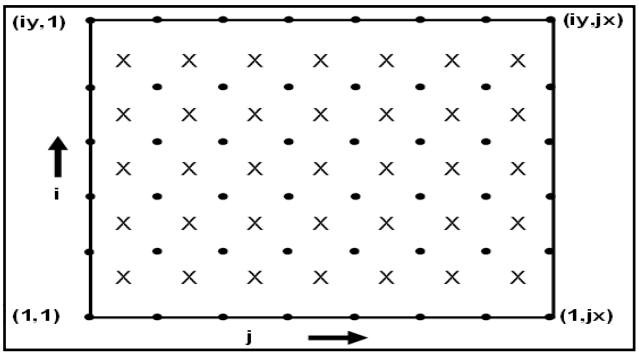

Fig (13): Representation the horizontal dot and cross grid points.

It can be seen from the equation and Figure (12) that σ is zero at the top and one at the surface, and each model level is defined by a value of σ. The model vertical resolution is defined by a list of values between zero and one that do not necessarily have to be evenly spaced.

Commonly the resolution in the boundary layer is much finer than above, and the number of levels may vary upon the user demand. The horizontal grid has an Arakawa-Lamb B-staggering of the velocity variables with respect to the scalar variables. This is shown in Figure (13) where it can be seen that the scalars (T, q, p, etc.) are defined at the center of the grid box, velocity is defined at dot points. While the eastward (u) and northward (v) velocity components are collocated at the corners. The center points of grid squares will be referred to as corner points are dot points. Hence horizontal velocity is defined at dot points. Data is input to the model, the preprocessors do the necessary interpolation to assure consistency with the grid.

All the above variables are defined in the middle of each model vertical layer, referred to as half-levels and represented by the dashed lines in Figure (12). Vertical velocity is carried at the full levels (solid lines). In defining the sigma levels it is the full levels that are listed, including levels at σ = 0 and 1. The number of model layers is therefore always one less than the number of full sigma levels. The finite differencing in the model is, of course, crucially dependent upon the grid staggering wherever gradients or averaging are represented terms in the equation.

Available Studies Concerning Blocking Systems

The term blocking was first introduced into synoptic meteorology in American Publications to define a particular type of tropospheric flow. A good deal of literature concerning blocking is now available to the extent that the word itself is now a widely accepted term in the standard nomenclature of meteorology. Presently, the increase in aerological data has enabled not only an increased examination of this phenomenon, but also the effect of this phenomenon on a weather and climate.

Since a long time Namias, (1947). Described blocking in terms of retardation (diminution) of the zonal circulation in a limited sector of the hemisphere at all levels within the troposphere.

Berggren, Bolin and Rossby (1949), almost accept Namias's definition that retrogression is included. They attempt some sort of explanation of the initiation and development of blocking in terms of instabilities in the normal zonal circulation, leading to abnormal growth of upper waves and to partial cutting off of warm anticycolonic and cold cyclonic vortices by a sort of large scale seclusion process.

Elliott and smith (1949), Define the blocking as a state of circulation in which the normal zonal flow is interrupted in a sector, by strong persistent, meridional-type flow. Synoptically, a persistent high pressure at high latitudes abstracting the normal is toward progress of migratory cyclones and anticyclones. The high is linked, as a rule, to simultaneous abnormally deep depression either upstream or downstream or both, which are often trapped in low latitudes.

Rex, (1950a), pointed that a case of blocking should exhibit the flowing characteristics: The basic westerly current must split into two branches. Each branch current must transport an appreciable mass. The double-jet system must extend over at least 450 longitudes. A sharp transition from zonal type flow up stream to meridional type downstream must be observed across the current split. The pattern must persist with recognizable continuity for at least ten days.

Rex, (1950b), attains the following results: Blocking action is most frequently initiated in two relatively narrow longitudinal zones in the Northern Hemisphere, one (Atlantic) centered a loft at 100 West longitudes while the other (Pacific) centered at 1500 West longitude.

Rex, (1950 a, b), Examined the Northern Hemisphere daily 500mb flow patterns, 3km and surface charts for 19 years (1932 - 1950) to afford a catalogue of blocking events. He showed that the occurrence of blocking has two outstanding locations. The Atlantic blocking (600 W - 200 E) and the Pacific blocking (1800 W - 1200 W) 82 occurrences of Atlantic blocking and 30 of Pacific blocking were available. He showed that for both the Pacific and Atlantic, the maximum occurs in April-May (23% for the Pacific and 40% for the Atlantic), and the minimum occurrence happened to be in August-September. The summer minimum for the Pacific was zero, while for the Atlantic the summer minimum was ~ 15%.

Everson and Davis, (1970) and Kikuchi (1971), they run numerical experiments with quasi-geostrophic model in order to look the blocking phenomenon. Both found that a persistent blocking appears almost only when geography or land-sea contrast are incorporated into the model.

Egger, (1979), uses a barotropic channel to show the characteristic feature of atmospheric blocking. The blocks are created and maintained through the interaction of forced waves with slowly moving free waves. It is found that zonal wind profiles with a jet at the channel axis are not favorable for blocking whereas a double jet structure enhances blocking activity the influence on the blocking process is not strong but generally stabilizing.

Dennis and Ghan, (1980), made an objective method showing that the vorticity budgets and heat budgets of the blocking ridge cases are compared statistically with those of transient ridges for both the Pacific and Atlantic oceanic region. It is demonstrated that there are statistically significant differences in the vorticity and heat budgets of blocking compared to transient ridges in zonal advection.

Charny, et. al., (1981), suggested that the generation and decay of blocks may occur by change of external factors dividing the flow closer to or farther from topographic resonance, or by strong, large-scale cyclonic development.

Dole, (1982), calculated the frequencies of persistent anomalies by using 14 years winter 500gph heights data. He found three major favorable regions for the occurrence of persistent anomalies, the North Pacific, the North Atlantic and North of former Soviet Union. For each region the maximum frequency of occurrence of positive anomalies and negative anomalies coexisted and had comparable magnitudes.

Hans's okland and Harald lejenas, (1986), Time series of observational data have been used to study persistence of blocking over the Atlantic (Northern Hemisphere) and over the Australian-New Zealand region. The data used are 500gph geopotential height data. It is shown that the probability that a blocking episode, which has prevailed for I days, will exist day I + 1 is ca 0.7 for Northern Hemisphere blocking and ca 0.5 for Southern Hemisphere blocking. The probability increase somewhat the longer the episode lasts. It is demonstrated that the statistics nevertheless may be modeled as a first order Markov process.

Frederiksen and Ball, (1989), have studied the role of instability during the onset of blocking and cyclogenesis in the Northern Hemisphere synoptic flows using a sequence of daily instantaneous atmospheric flows. They also analyzed the adjoined instability eigenmodes and have argued, on the basis of these, that the cyclogenesis modes can trigger events that can lead to the formation of mature blocking.

Hafez y.y. (1995), the effect of blocking highs over Eastern Europe on weather in Egypt during winter concludes that weather in Egypt is highly controlled by successive blocking highs persisting over Eastern Europe during winter seasons. In other words, weather in Egypt is influenced by the number of occurrence of blocking highs over Eastern Europe which persist more than or equal seven days in winter.

Tsou and Smith, (1998), founded that energy transformation associated with a wave system that included the development of a blocking anticyclone over the North Atlantic Ocean and the upstream explosive-development of extratropical cyclones are studied for the period 17–21 January 1979. Included in the investigation are eddy kinetic energy (KE), release of eddy potential energy (CE), generation of eddy kinetic energy (GK), and the exchange between eddy and zonal kinetic energy (CK).

Hansen and sutera, (1993), they found that, by using the observations of 500gph data from 28 North Hemisphere winters found that most European blocking episodes (78 %) are a part of an amplified wave flow regime during some part of their life cycle. Blocking in this sector developed along with or during an amplified wave regime in 30 of 51 cases.

Lupo and Smith, (1994), use of 3-year climatology of North Hemisphere blocking was developed using ECMWF analysis to drive a comprehensive set of blocking anticyclone characteristics, included location, frequency, duration, intensity, size, seasonal, and regional distribution, and relationship to precursor cyclones and jet streaks.

Hafez, (1995), study the effect of blocking highs over Eastern Europe on weather in Egypt is highly controlled by successive blocking highs persisting over Eastern Europe during winter seasons. In other words, weather in Egypt is influenced by the number of occurrence of blocking highs over Eastern Europe which persist ≥ 7 days in winter.

Pelly and Hoskins, (2002) they found that, it is argued that the essential aspect of atmospheric blocking may be seen in the wave breaking of potential temperature (θ) on a potential vorticity (pv) surface, which may identified with the tropopause, and the consequent reversal of the usually meridional temperature gradient of θ.

Hasanean and Hafez, (2003), they make attempts to find a physical solution for the blocking formation. In order to study the occurrence of splitting in westerly air current, the equation of motion in natural coordinate system was used.

Lupo et.al, (2007) in this study depend on number of blocking cases from (1970-2006) around the global, where found that the number of blocking cases which occurrences in Northern Hemisphere more than the number of blocking cases which occurrences in Southern Hemisphere, but the blocking cases in Southern Hemisphere are more sever in weather change about occurrences in Northern Hemisphere, and found relationship between blocking cases and ElNino and LaNina.

Results and Discussions

Initially we will take data of 1200 UTC 500mb daily geopotential height charts from (1995-2005) eleven year from National Oceanic and Atmospheric Administration (NOAA) web site (http://www.cdc.noaa.gov/Composites/Day/). According to definition of Blocking in introduction, we will separating the blocking cases which occurs in the range from (1995 –2005) 1200 UTC 500mb under three conditions as follow:-

1- according to splitting of westerlise.
2- according to the shape of (Diffluent, Omega, Meridional) blocks.
3- according to the condition of persistence ≥ 5 days.

From output data we get on 32 cases as shown in table (1) and we will chose from winter season one case occur in Jan 2001 which persist 7 days in this study.

Table (1): Blocking Case in Winter which Persistence ≥ 5 Days From (1995–2005)

Persistence by days	Winter	Spring	Summer	Autumn
≥ 5 days	17	5	5	5

According to the definitions, properties and putted conditions for horizontal and vertical distribution of using model {Regional Climate Model version three (RegCM3)} which refer to it in introduction, and after finished from RUN with settings horizontal resolution of (100 km) for data years from (1995–2005) 1200 UTC 500mb.

We will take one case occur in winter season and compare the properties of this actual charts according to the centers of Lows and Highs and pressure values of each them as in tables (2,3) with output RUN charts of the same days which called Estimated, and calculate the absolute percentage error between actual and estimated charts of horizontal resolution (100 km), also absolute percentage error in pressure values between them and then calculate the accuracy percentage of this model in winter season until known the efficiency of this model and the resolution in simulation of blocking phenomena in winter season. From tables (2 and 3), we notice that, the

absolute error varies from 0.4 to 2.2% between the actual and estimated pressure in the first and second low, while varies from 0.5 to 12.4 in first high and second high. This due to the differences in the pressure for actual and estimated values in first and second high is greater than in the first and second low.

Table (2): The centers of First (Low, High) and pressure values for Actual and Estimated Charts (RUN-100Km) of 1200h, 500hPa in Winter case Jan (2001)

Date of case	$F.L_{Act.}$			$F.L_{Est.}$			$F.H_{Act.}$			$F.H_{Est.}$		
	$C.F.L_{Act.}$		P.V $FL_{Act.}$	$C.F.L_{Est.}$		P.V $FL_{Est.}$	$C.S.H_{Act.}$		P.V $FH_{Act.}$	$C.S.H_{Est.}$		P.V $FH_{Est.}$
D/M/Y	Lat.	Long.		Lat.	Long.		Lat.	Long.		Lat.	Long.	
10/01/01	47	-20	5420	50	-12	5360	60	-20	5500	61	-15	5440
11/01/01	45	-12	5460	42	4	5540	60	-15	5580	57	-8	5560
12/01/01	37	-5	5500	37	5	5440	57	-4	5660	33	-25	5800
13/01/01	35	7	5480	41	11	5360	58	3	5720	43	-20	5840
14/01/01	63	-45	5000	65	-38	4920	57	7	5720	37	-19	5880
15/01/01	67	-50	4990	67	-48	5000	55	7	6670	37	-25	5840
16/01/01	67	-47	4910	67	-44	5000	57	10	5630	35	-35	5880

Table (3): The centers of Second (Low, High) and pressure values for Actual and Estimated Charts (RUN-100Km) of 1200h, 500hPa in Winter case Jan (2001)

Date of case	$S.L_{Act.}$			$S.L_{Est.}$			$S.H_{Act.}$			$S.H_{Est.}$		
	$C.S.L_{Act.}$		P.V SL_{AC}	$C.S.L_{Est.}$		P.V SL_{ES}	$C.S.H_{Act.}$		P.V SH_{AC}	$C.S.H_{Est.}$		P.V $SH_{Est.}$
D/M/Y	Lat.	Long.		Lat.	Long.		Lat.	Long.		Lat.	Long.	
10/01/01	65	25	5140	65	25	5120	43	52	5680	47	65	5640
11/01/01	60	30	5140	57	27	5120	45	70	5620	45	70	5600
12/01/01	60	45	5140	57	38	5160	40	75	5620	43	75	5600
13/01/01	54	45	5120	67	65	5200	40	75	5640	35	70	5600
14/01/01	36	16	5480	37	8	5400	52	51	5160	56	60	5120
15/01/01	35	7	5550	37	5	5400	48	58	5150	48	65	5080
16/01/01	47	-2	5470	37	5	5440	65	70	5130	48	65	5080

Table keys

$F.L_{Act.}$	First Low Actual.	$C.S.H_{Act.}$	Center of Second High Actual.
$F.L_{Est.}$	First Low Estimated.	$C.S.H_{Est.}$	Center of Second High Estimated.
$F.H_{Act.}$	First High Actual.	Lat.	Latitude.
$F.H_{Est.}$	First High Estimated.	Long.	Longitude.
$S.L_{Act.}$	Second Low Actual.	P.V- $FL_{Act.}$	Pressure Value at First Low Actual.
$S.H_{Est.}$	Second High Estimated.	P.V- $FL_{Est.}$	Pressure Value at First Low Estimated.
$C.F.L_{Act.}$	Center of First Low Actual.	P.V- $FH_{Act.}$	Pressure Value at First High Actual.
$C.F.L_{Est.}$	Center of First Low Estimated.	P.V- $FH_{Est.}$	Pressure Value at First High Estimated.
$C.S.L_{Act.}$	Center of Second Low Actual.	P.V- $SL_{Act.}$	Pressure Value at Second Low Actual.
$C.S.L_{Est.}$	Center of Second Low Estimated.	P.V- $SL_{Est.}$	Pressure Value at Second Low Estimated.
$C.F.H_{Act.}$	Center of First High Actual.	P.V- $SH_{Act.}$	Pressure Value at Second High Actual.
$C.F.H_{Est.}$	Center of First High Estimated.	P.V- $SH_{Est.}$	Pressure Value at Second High Estimated.

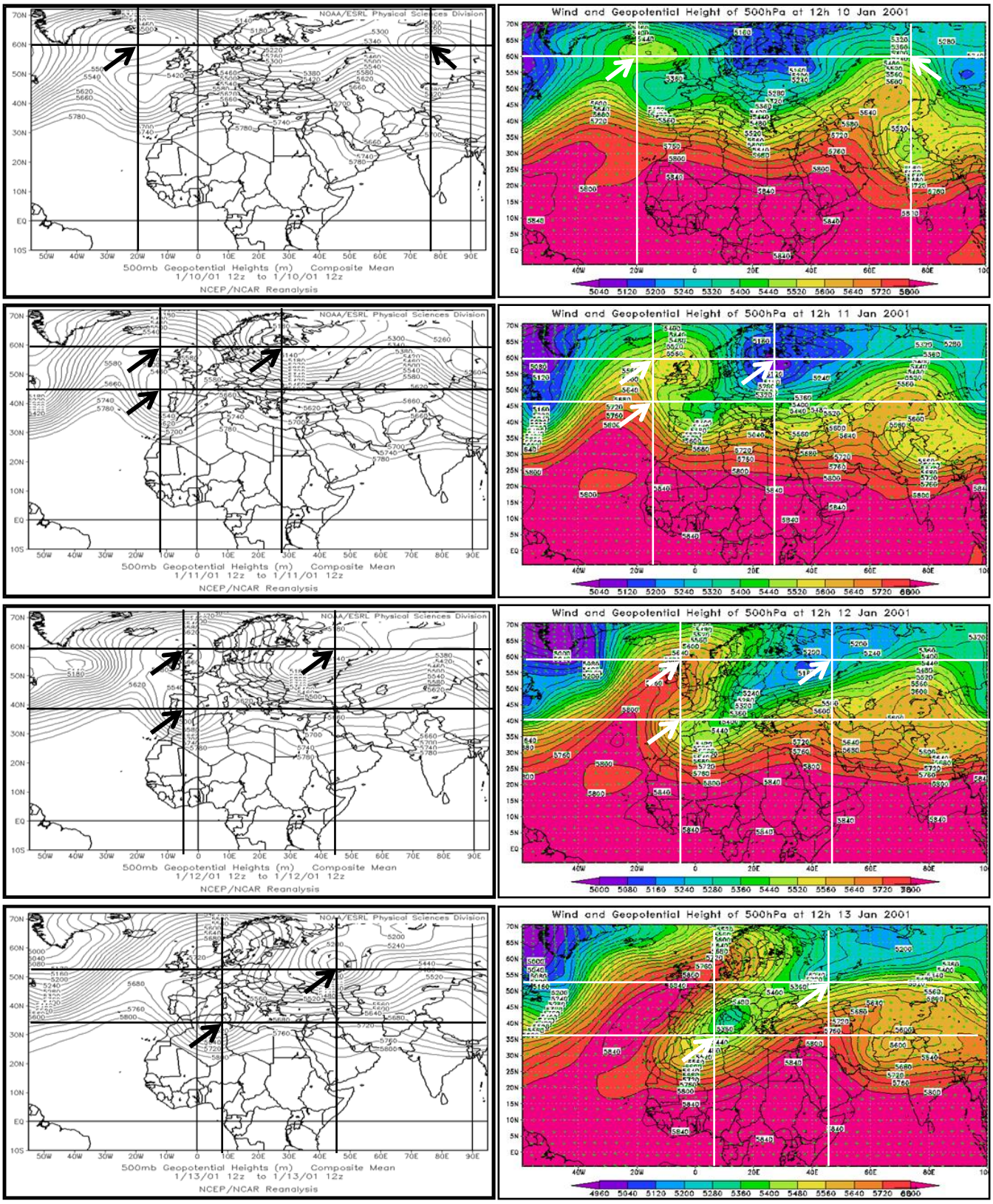

Fig (14): The actual and estimated charts in winter season

Actual Charts of case Jan-2001 **Estimated Charts of case Jan-2001**

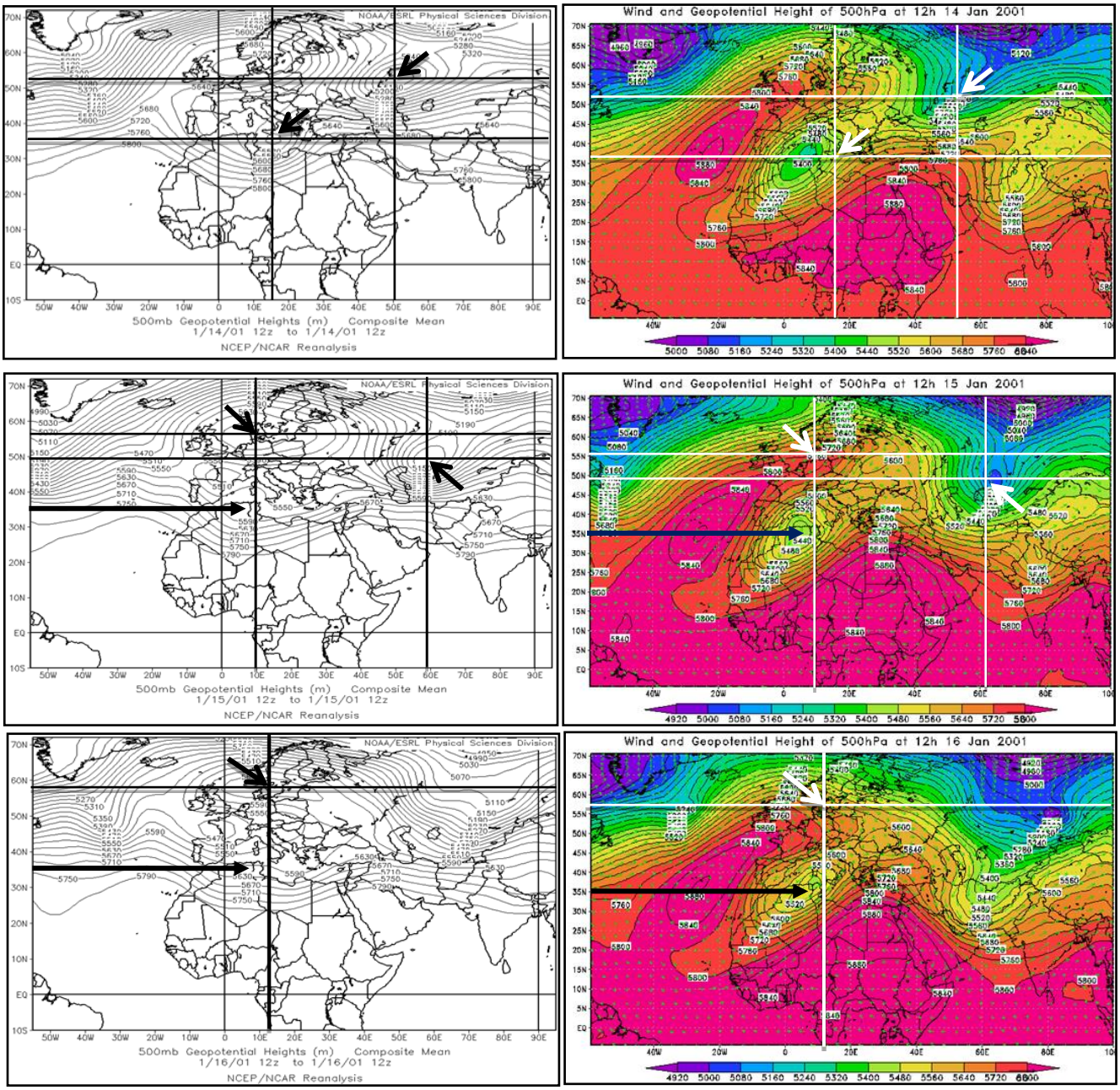

Fig (14): Cont.

Figure (14): show that the actual and estimated charts in the present work during winter season, from this figure we notice that in 10–Jan the center of low at the left (GMT) on the actual charts differs from estimated charts by three degrees of longitude, while the second low 10 degrees longitude with stability Latitude each another them. In 11-Jan one of the more accurate days in simulated estimated chart compare with the actual chart, but in 12–Jan the best representation of the reality on low (60^0N-45^0E), while in 13–Jan there is a difference in the change of Contour Lines shape between actual and estimated charts, in this day creating a difference in issuing forecasts on these areas. The maps estimated give southerly winds on north-west Egypt, while in actual charts gives this prediction on the north-west to Libya, Tunisia, Algeria and Morocco, which continued at the same case for the next day (14 – Jan).

Also in 15–Jan remained estimated charts give the same prediction of the previous days (pressure value 5440 mb), despite the erosion of the existence of this low on actual charts (pressure value 5590 mb), this mean 150mb difference between them, which continued at the same case for the next day (16–Jan). From the above discussion, it is clear that, the simulation model at the beginning of the situation was better than the end of this case.

In another hand in (Mar-2005) represent the Spring season and investigation the properties of the actual charts according to the centers of Lows and Highs and pressure values of each them as in tables (4,5) with output RUN charts of the same days which called Estimated, and calculate the error between actual and Estimated charts, also calculate the absolute percentage error in pressure values between them and then calculate the accuracy percentage of this model in spring season until known the efficiency this model and this resolution in simulation of blocking phenomena in spring. From tables (4 and 5), we notice that, the absolute error varies from (0.8 to 4.7) % between the actual and estimated pressure in the first and second low, while slightly varies between the first and second high. This due to the not differences in the pressure for actual and estimated values in first and second high is greater than in the first and second low.

Table (4): The centers of First (Low, High) and pressure values for Actual and Estimated Charts (RUN-100Km) of 1200h 500hPa in Spring case Mar (2005)

Date of case	$F.L_{Act.}$			$F.L_{Est.}$			$F.H_{Act.}$			$F.H_{Est.}$		
	$C.F.L_{Act.}$		P.V $FL_{Act.}$	$C.F.L_{Est.}$		P.V $FL_{Est.}$	$C.F.H_{Act.}$		P.V FH_{Act}	$C.F.H_{Est.}$		P.V $FH_{Est.}$
D/M/Y	Lat.	Long.		Lat.	Long.		Lat.	Long.		Lat.	Long.	
24/03/05	44	-28	5240	40	-30	5340	50	10	5640	52	8	5640
25/03/05	46	-25	5320	45	-28	5400	50	10	5600	50	10	5640
26/03/05	47	-20	5400	47	-25	5480	62	-10	5560	59	-15	5560
27/03/05	63	-53	5160	65	-53	5080	64	-10	5600	63	-15	5600
28/03/05	43	-43	5480	45	-45	5480	65	-5	5600	65	-15	5600

Table (5): The centers of Second (Low, High) and pressure values for Actual and Estimated Charts (RUN-100Km) of 1200h 500hPa in Spring case Mar (2005)

Date of case	$S.L_{Act.}$			$S.L_{Est.}$			$S.H_{Act.}$			$S.H_{Est.}$		
	$C.S.L_{Act.}$		P.V $SL_{Act.}$	$C.S.L_{Est.}$		P.V $SL_{Est.}$	$C.S.H_{Act.}$		P.V $SH_{Act.}$	$C.S.H_{Est.}$		P.V $SH_{Est.}$
D/M/Y	Lat.	Long.		Lat.	Long.		Lat.	Long.		Lat.	Long.	
24/03/05	75	65	5080	65	73	5040	0	0	0	0	0	0
25/03/05	45	60	5360	37	30	5360	0	0	0	0	0	0
26/03/05	53	67	5160	35	35	5400	0	0	0	0	0	0
27/03/05	63	46	5120	58	50	5080	0	0	0	0	0	0
28/03/05	57	45	5120	57	50	5080	0	0	0	0	0	0

Actual Charts of case Mar-2005 **Estimated Charts of case Mar-2005**

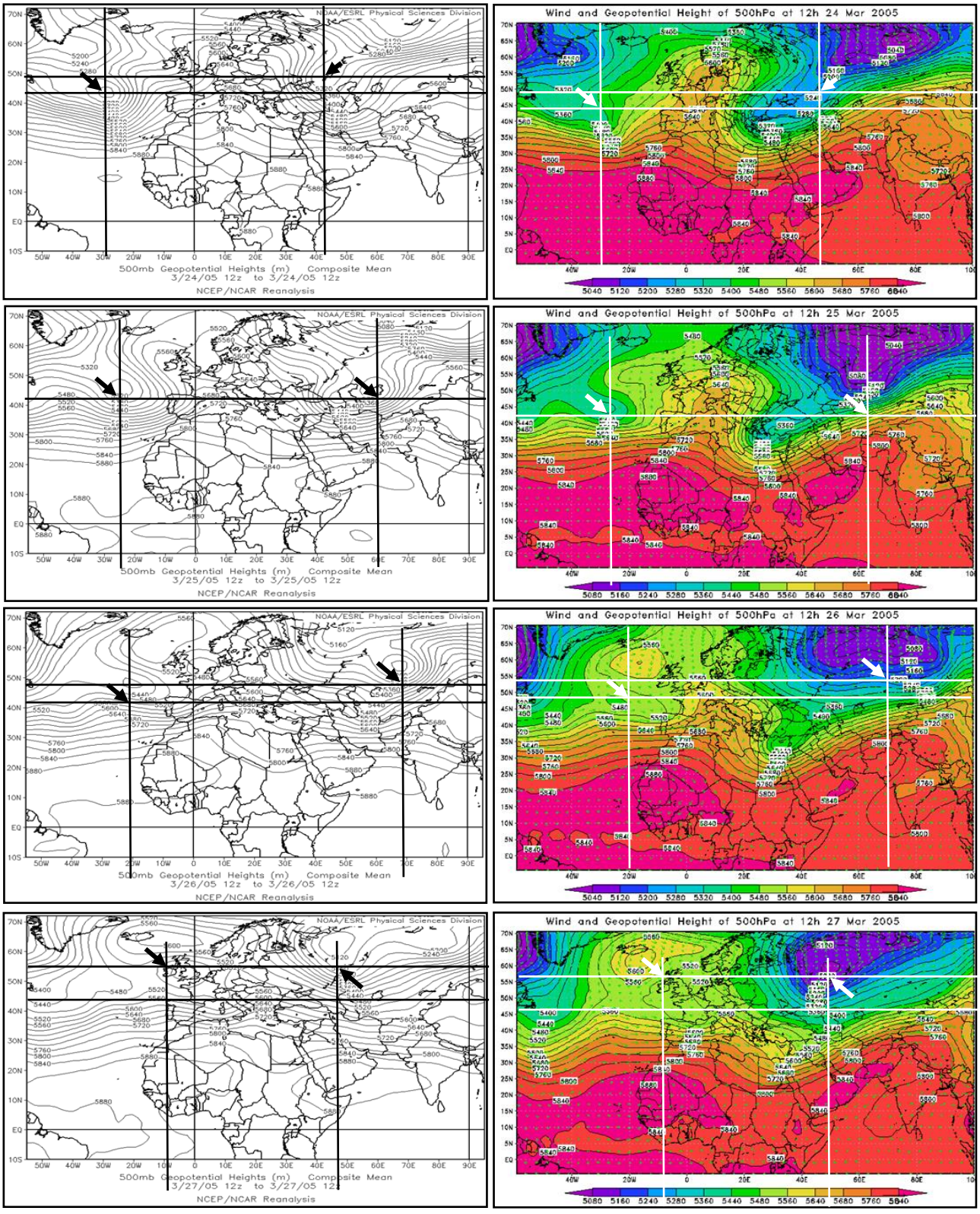

Fig (15): The actual and estimated charts in spring season

Actual Charts of case Mar-2005 **Estimated Charts of case Mar-2005**

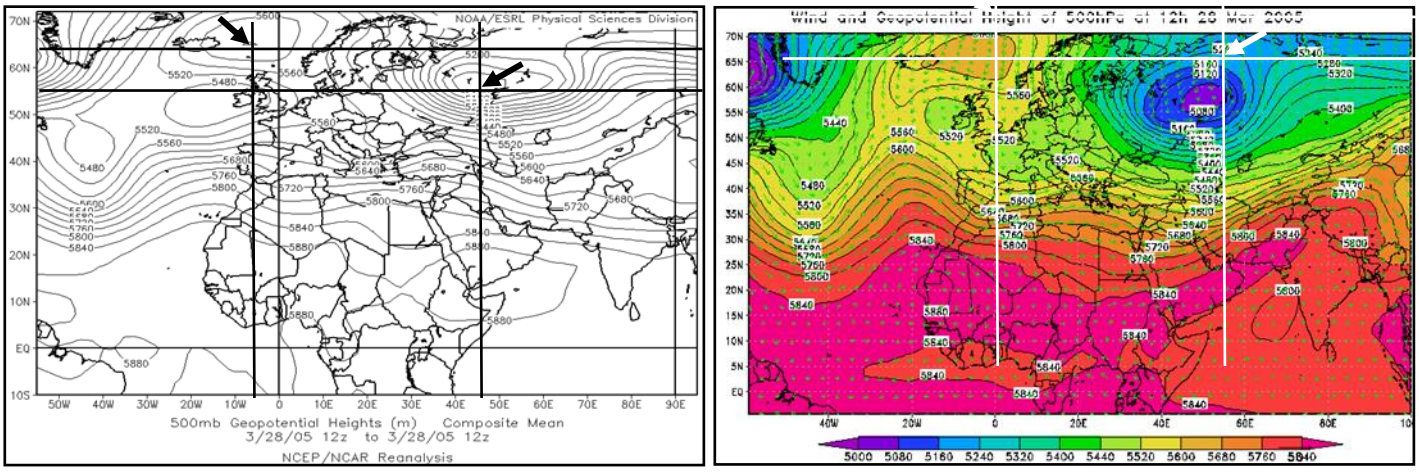

Fig (15): Cont.

In each of Mar was 24-25 estimated charts simulate actual by as much as approximately 94%, while in the 26-27 Mar estimated chart indicated that the presence of a depression hit the northeast coast of Egypt and the Sinai region, while fading in actual chart. It returned on 28-Mar to reach for the same percentage mentioned in the simulation. The spring is the best representation for winter.

Table (6): The centers of First (Low, High) and pressure values for Actual and Estimated Charts (RUN-100Km) of 1200h 500hPa in Summer case Jun (2001)

Date of case	$F.L_{Act.}$			$F.L_{Est.}$			$F.H_{Act.}$			$F.H_{Est.}$		
	$C.F.L_{Act.}$		P.V $FL_{Act.}$	$C.F.L_{Est.}$		P.V $FL_{Est.}$	$C.S.H_{Act.}$		P.V FH_{Act}	$C.F.H_{Est.}$		P.V FH_{Est}
D/M/Y	Lat.	Long.		Lat.	Long.		Lat.	Long.		Lat.	Long.	
19/06/01	40	-30	5540	47	-33	5580	45	-5	5880	45	-5	5840
20/06/01	42	-33	5610	52	-22	5520	45	-8	5850	52	-5	5840
21/06/01	48	-33	5550	45	-25	5560	45	-8	5870	48	5	5800
22/06/01	55	-40	5510	57	-38	5480	40	-5	5870	50	15	5800
23/06/01	55	-28	5500	57	-33	5480	65	-5	5870	47	15	5840

Table (7): The centers of Second (Low, High) and pressure values for Actual and Estimated Charts (RUN-100Km) of 1200h 500hPa in Summer case Jun (2001)

Date of case	$S.L_{Act.}$			$S.L_{Est.}$			$S.H_{Act.}$			$S.H_{Est.}$		
	$C.S.L_{Act.}$		P.V $SL_{Act.}$	$C.S.L_{ES}$		P.V $SL_{Est.}$	$C.S.H_{Act.}$		P.V $SH_{Act.}$	$C.S.H_{Est.}$		P.V $SH_{Est.}$
D/M/Y	Lat.	Long.		Lat.	Long.		Lat.	Long.		Lat.	Long.	
19/06/01	42	23	5600	45	25	5680	52	37	5760	50	50	5800
20/06/01	45	25	5610	40	25	5720	50	40	5770	55	55	5760
21/06/01	47	27	5630	55	30	5600	50	45	5790	45	60	5800
22/06/01	55	15	5510	53	43	5620	50	50	5790	52	65	5720
23/06/01	53	25	5505	55	52	5580	40	55	5865	50	69	5720

For summer season, case of (Jun-2001) and compare by the same previous method as in data in tables (6, 7). The error between actual and estimated charts of horizontal resolution (100 km) and pressure values between them also calculate the accuracy percentage in simulation of blocking phenomena of this model in summer we will know.

Actual Charts of case Jun-2001 **Estimated Charts of case Jun-2001**

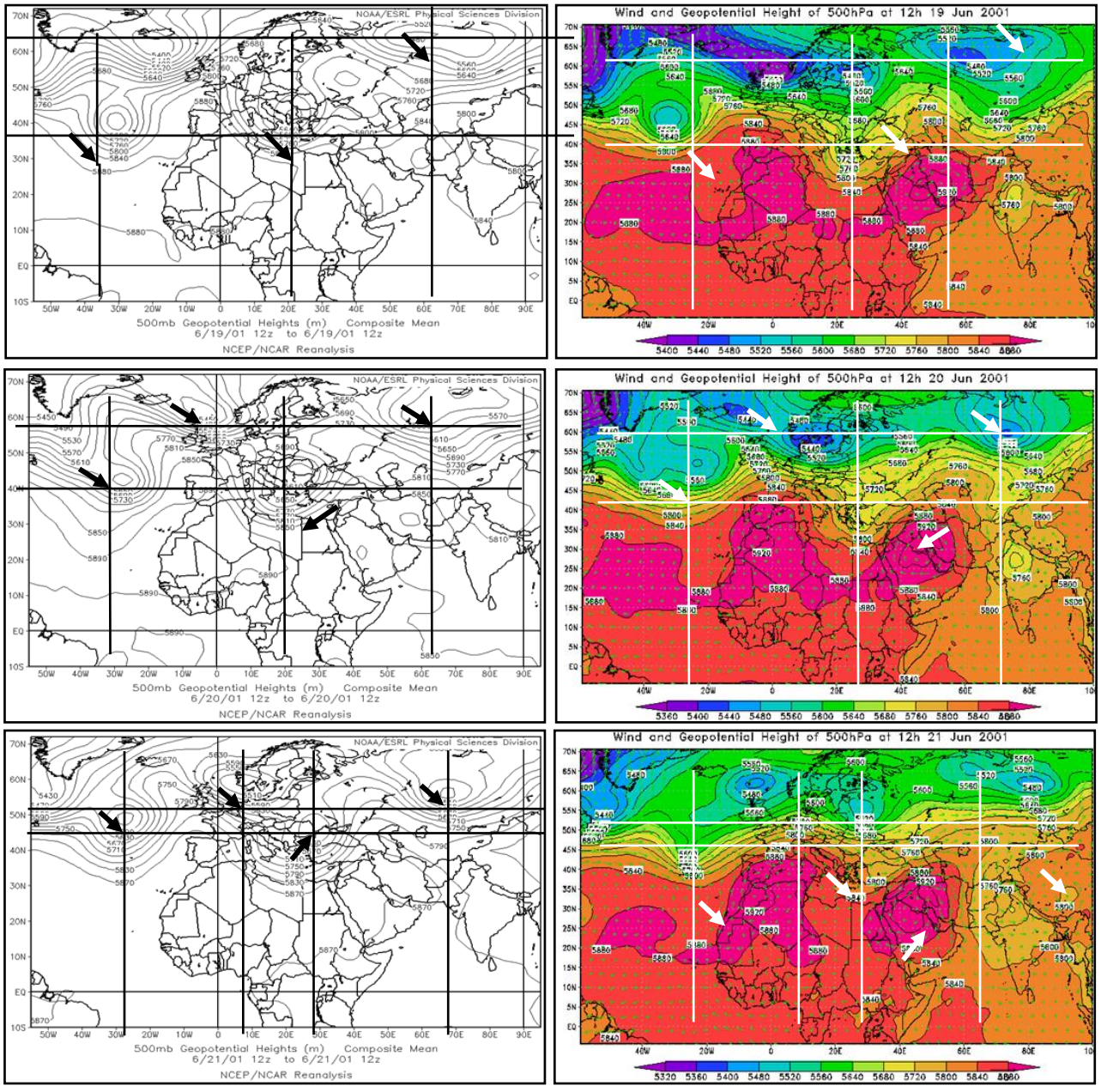

Fig (16): The actual and estimated charts in summer season

Actual Charts of case Jun-2001 **Estimated Charts of case Jun-2001**

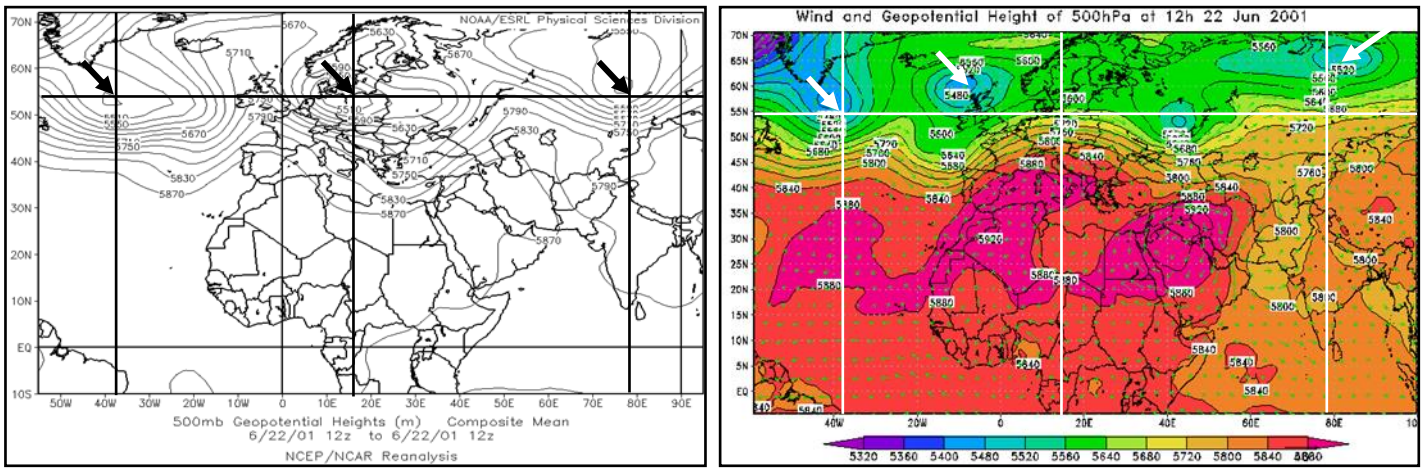

Fig (16): Cont.

From tables (6 and 7), it is clear that, the absolute error varies from (0.2 to 1.6) % between the actual and estimated pressure in the first and second low, while varies from (0.2 to 2.8) % between the first and second high.

Figure (16), show the actual and estimated charts in summer season. From this figure, we noticeable that, in 19-06-2001 actual charts show that, a low pressure on Italy and extends its influence to the northern coast of Libya, while each differed the center of rotation and its influence on the North West coast of Egypt in estimated charts but on 20-06-2001 deepen previous low in actual charts while completely fading influence in estimated charts, and in 21-06-2001 clarified actual charts be high pressure between the low pressure on the (27^0 W – 50^0 N) and the second on (8^0 E – 56^0 N), while fading completely in estimated charts, and extended it until the day 22/06/2001 but on 23-06-2001 the actual charts show that deeping of low pressure in (26^0 E – 52^0 N), while on the same position in estimated charts give high pressure, from above result we conclude that, the summer season give the worst representation in the simulation of reality.

Table (8): The centers of First (Low, High) and pressure values for Actual and Estimated Charts (RUN-100Km) of 1200h, 500hPa in Autumn case Sep (2005)

Date of case	$F.L_{Act.}$			$F.L_{Est.}$			$F.H_{Act.}$			$F.H_{Est.}$		
	$C.F.L_{Act.}$		P.V $FL_{Act.}$	$C.F.L_{Est.}$		P.V $FL_{Est.}$	$C.F.H_{Act.}$		P.V $FH_{Act.}$	$C.F.H_{ES}$		P.V $FH_{Est.}$
D/M/Y	Lat.	Long.		Lat.	Long.		Lat.	Long.		Lat.	Long.	
02/09/05	52	-25	5520	65	-20	5400	63	25	5840	57	30	5840
03/09/05	50	-20	5600	45	-20	5760	55	15	5840	55	33	5800
04/09/05	48	-12	5600	45	-15	5760	53	13	5840	53	30	5720
05/09/05	50	-8	5640	40	-14	5720	52	12	5800	45	15	5680
06/09/05	53	-3	5640	38	-22	5720	53	18	5800	50	30	5640

Table (9): The centers of Second (Low, High) and pressure values for Actual and Estimated Charts (RUN-100Km) of 1200h 500hPa in Autumn case Sep (2005)

Date of case	$S.L_{Act.}$			$S.L_{Est.}$			$S.H_{Act.}$			$S.H_{Est.}$		
	$C.S.L_{Act.}$		P.V $SL_{Act.}$	$C.S.L_{Est.}$		P.V $SL_{Est.}$	$C.S.H_{Act.}$		P.V $SH_{Act.}$	$C.S.H_{Est.}$		P.V $SH_{Est.}$
D/M/Y	Lat.	Long.		Lat.	Long.		Lat.	Long.		Lat.	Long.	
02/09/05	58	50	5560	58	60	5600	0	0	0	0	0	0
03/09/05	55	55	5600	52	58	5540	0	0	0	0	0	0
04/09/05	57	57	5520	49	59	5580	0	0	0	0	0	0
05/09/05	57	63	5480	47	65	5520	0	0	0	0	0	0
06/09/05	60	70	5440	54	70	5520	0	0	0	0	0	0

For autumn season, case of (Sep-2005) and compare the properties of this actual charts according to the centers of Lows and Highs and pressure values of each them as in tables (8,9) with output RUN charts of the same days which called Estimated, and calculate the error between actual and Estimated charts of horizontal resolution (100 km) also calculate the Error Percentage in pressure values between them and then calculate the accuracy percentage of this model in Autumn season until known the efficiency this model and this resolution in simulation of blocking phenomena in autumn. From tables (8 and 9), we notice that, the absolute error varies from (0.7 to 2.9) % between the actual and estimated pressure in the first and second low, while slightly varies between the first and second high.

The actual and estimated charts in autumn season show in Figure (17), in autumn on 02-09-2005. The comparison between the actual and estimated charts show simple change between the centers of spins, whether high or low pressure range (10-30) in the longitude and stability of latitude, and extended it until the next day 03-09-2005, in 04-09-2005. The comparison between the actual and estimated charts show that the center of low in actually on (57^0 E – 57^0 N) while in estimated on (57^0 E – 50^0 N) a difference of approximately 7^0 degree in latitude at the same longitude, and extended it influence to include the next day respectively 05-09-2005, while in 06-09-2005. The comparison between the actual and estimated charts show that the center of low in actually on (71^0 E – 59^0 N) while in estimated on (71^0 E – 52^0 N) a difference of approximately 7^0 degree in latitude at the same longitude.

Actual Charts of case Sep-2005 **Estimated Charts of case Sep-2005**

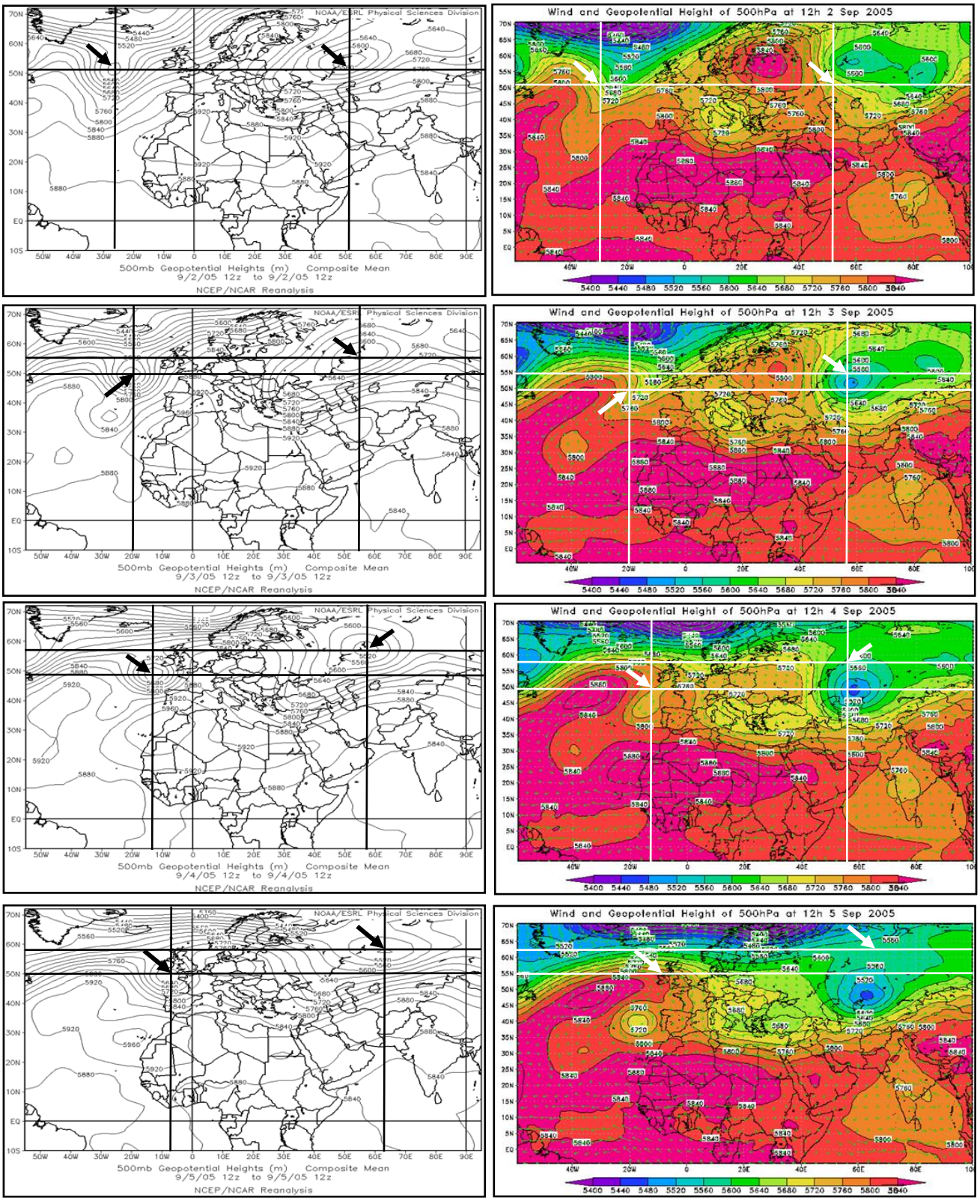

Fig (17): The actual and estimated charts in autumn season

Actual Charts of case Sep-2005 **Estimated Charts of case Sep-200**

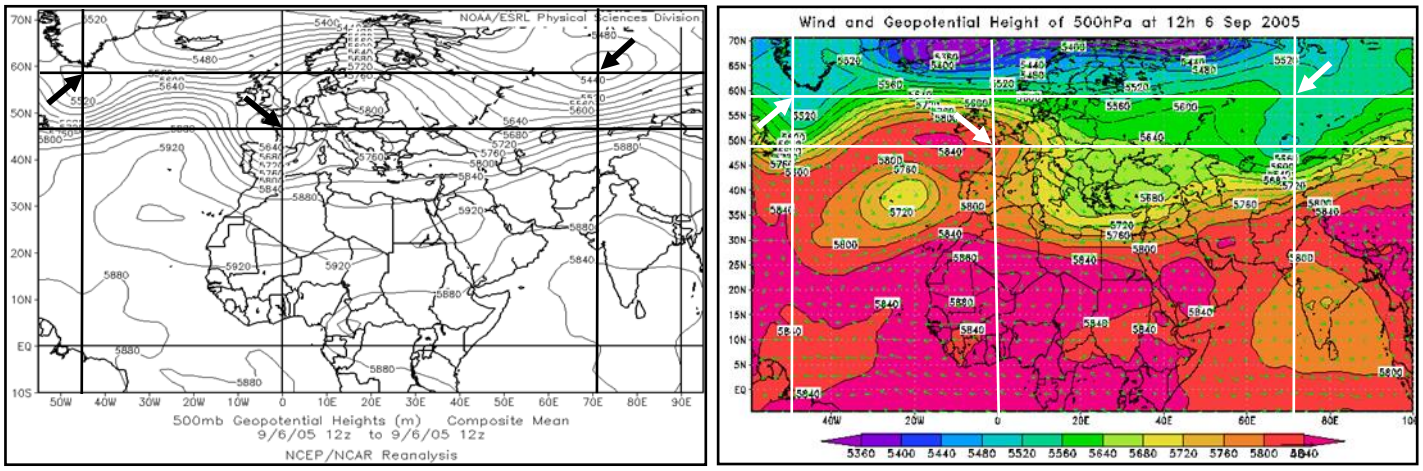

Fig (17): Cont.

Conclusion

In winter season, the absolute error varies from 0.4 to 2.2% between the actual and estimated pressure in the first and second low, while varies from 0.5 to 12.4 in first high and second high. This due to the differences in the pressure for actual and estimated values in first and second high is greater than in the first and second low. While in spring season the absolute error varies from (0.8 to 4.7) % between the actual and estimated pressure in the first and second low, while slightly varies between the first and second high. This due to the not differences in the pressure for actual and estimated values in first and second high is greater than in the first and second low. But in summer season the absolute error varies from (0.2 to 1.6) % between the actual and estimated pressure in the first and second low, while varies from (0.2 to 2.8) % between the first and second high, and in autumn season the absolute error varies from (0.7 to 2.9) % between the actual and estimated pressure in the first and second low, while slightly varies between the first and second high.

Generally, from the above results and compared between the actual and estimated charts by using $RgCM_3$ horizontal resolution 100km, we can order the different seasonal according to the accuracy: spring, winter, autumn and summer seasons. This means that, the simulation of blocking systems using of limited area model (RegCM3) will clarify the role played by blocking systems in abnormal weather and eliminate the hazards of the sever abnormal weather phenomena which related to blocking systems.

References

Anthes, R. A., 1977: A cumulus parameterization scheme utilizing a one-dimensional cloud model, Mon. Wea. Rev., 105, 270–286.

Berggren, R., Bolin, B. and Rossby, C. G. (1949): An aerological study of zonal motion, its perturbations and breakdown. Tellus 1, 2, 14-37.

Briegleb, B. P., (1992): Delta-eddington approximation for solar radiation in the ncar community climate model, J. Geophys. Res., 97, 7603–7612.

Charney, J. G. Shukla, J. and Mo, K.C. (1981), Comparison of a barotropic blocking theory with observation, J. Atmos. Sci., 38, 762-779.

Davies, H. C., and R. E. Turner, (1977): Updating prediction models by dynamical relaxation: An examination of the technique, Quart. J. Roy. Met., Soc., 103, 225–245.

Deardoff, J. W., (1978): Efficient prediction of ground surface temperature and moisture with inclusion of a layer of vegetation, J. Geophys. Res., 83, 1889 – 1903.

Dennis, L.H. and Steven, J.G. (1980), A statistical study of the dynamics of blocking. Mon. Wea. Rev., 108, 1144-1159.

Dickinson, R. E., R. M. Errico, F. Giorgi, and G. T. Bates, (1989): A regional climate model for the western United States, Climatic Change, 15, 383–422.

Dickinson, R. E., P. J. Kennedy, A. Henderson-Sellers, and M. Wilson, (1986): Biosphere-atmosphere transfer scheme (bats) for the ncar community climate model, Tech. Rep. NCARE/TN- 275+STR, National Center for Atmospheric Research.
Dickinson, R. E., A. Henderson-Sellers, and P. J. Kennedy, (1993), Biosphere-atmosphere transfer scheme (bats) version 1e as coupled to the ncar community climate model, Tech. rep., National Center for Atmospheric Research.
Dole, R.M. (1982), Persistent anomalies of the extratropical Northern Hemisphere winter time circulation. PH.D. Thesis, Massachusetts institute of technology.
Egger, John. (1979), The Austrian Method. In Spadaro ed., 1979, Pp. 19–39. Egger J. (1978), Dynamics of blocking highs J. Atoms. Sci., 35, 1788-1801.
Elbern, H. and Speth, P. (1992), Energy of Rossby waves as a part of global atmospheric oscillations. Tellus, 45A, 168-192.
Elliott, R.D. and Smith, T.B. (1949), A study of the effects of large blocking highs on the general circulation in the Northern Hemisphere westerlies. J. Meteorol., 6, 67-85.
Emanuel K. A. (1991), A scheme for representing cumulus convection in large-scale models, J. Atmos. Sci., 48(21), 2313–2335.
Everson, P. J and Davies, D. R. (1970): On the use of a simple two-level model in general circulation studies, ' Quart. J. R. Met. Soc., 96, pp. 404-412.
Feudal I. and Shukla J. (2010): Influence of sea surface temperature on the European heat wave of 2003 summer, Part II: a modeling study. Clim. Dyn., doi 10.1007/s00382-010-2450789-z.
Francisco J., Michel D. and David B. (1998), North Atlantic wintertime intraseasonal variability and its sensitivity to GCM horizontal resolution. Tellus, 50A, 573-595.
Frederiksen, J.S. (1978), Instability of planetary waves and zonal flows on the regions of cyclogensis. Quart J. R. Met., Soc., 104, 841-872.
Frederiksen, J.S. (1979a), The effect of long planetary waves on the regions of cyclogenesis Linear theory. J. Atoms. Sic., 36, 195-204.
Frederiksen, J.S., and Bell (1989), The role of instability during the onset of blocking and cyclogenesis in the Northern Hemisphere synoptic flow. J. Atoms. Sic., 46, 1076-1812.
Fritsch, J. M., and C. F. Chappell, (1980): Numerical prediction of convectively driven mesoscale pressure systems part i: Convective parameterization, J. Atmos. Sci., 37, 1722–1733.
Giorgi, F., G. T. Bates, and S. J. Nieman, (1993a): The multi-year surface climatology of a regional atmospheric model over the western United States, J. Climate, 6, 75–95.
Giorgi, F., M. R. Marinucci, and G. T. Bates, (1993b): Development of a second generation regional climate model (regcm2) i: Boundary layer and radiative transfer processes, Mon. Wea. Rev., 121, 2794–2813.
Giorgi, F., X. Q. Bi, and Y. Qian, (2003a): Indirect vs. direct effects of anthropogenic sulfate on the climate of East Asia as simulated with a regional coupled climate-emistry/aerosol model, Climatic Change, 58, 345–376.
Giorgi, F., R. Francisco, and J. S. Pal, (2003b): Effects of a subgrid-scale topography and land use scheme on the simulation of surface climate and hydrology. Part 1: Effects of temperature and water vapor disaggregation, Journal of Hydrometeorology, 4, 317–333.
Grell, G. A., J. Dudhia, and D. R. Stauffer, (1994): Description of the fifth generation Penn State/NCAR Mesoscale Model (MM5), Tech. Rep. TN- 398+STR, NCAR, Boulder, Colorado, pp. 121.
Grell G., (1993), Prognostic evaluation of assumptions used by cumulus parameterizations, Mon. Wea. Rev., 121, 764–787.
Hack, J. J., B. A. Boville, B. P. Briegleb, J. T. Kiehl, P. J. Rasch, and D. L. Williamson, (1993), Description of the ncar community climate model (ccm2), Tech. Rep. NCAR/TN-382+STR, National Center for Atmospheric Research.
Hansen, A. R. and Chen, T. C. (1982), A spectral energetics analysis of atmospheric blocking. Mon. Wea. Rev., 110, 1146-1165.
Hansen, R. and Sutera, A. (1993), A comparison between planetary wave flow regimes and blocking. Tellus, 45A, 281-288.
Hansokland R., and Harald I. (1986), Blocking and persistence, Tellus 39 A, 33-38.
H.M. Hasanean and Y.Y. Hafez (2003), On the formation of blocking" Journal of Mausam, Vol. 54, No. 3, 739-742.
Henderson-Sellers, B., (1986): Calculating the surface energy balance for lake and reservoir modeling: A review, Rev. Geophys., 24(3), 625–649.
Holtslag A. A. M., E. I. F. de Bruijn and H. L. Pan, (1990): A high resolution air mass transformation model for short-range weather forecasting, Mon. Wea. Rev., 118, 1561–1575.
Holton (2004): J.R. An Introduction to Dynamic Meteorology, Elsevier Academic Press, 2004: 216.

Hostetler, S. W., G. T. Bates, and F. Giorgi, (1993): Interactive nesting of a lake thermal model within a regional climate model for climate change studies, Geophysical Research, 98, 5045–5057.
Hsie, E. Y., R. A. Anthes, and D. Keyser, (1984): Numerical simulation of frontogenisis in a moist atmosphere, J. Atmos. Sci., 41, 2581–2594.
Ji L. R. and Tibaldis S. (1982), Numerical simulations of a case of blocking: the effects of orography and land-sea contrast, ECMWF Tech. Rep. No. 33.
Kiehl, J. T., J. J. Hack, G. B. Bonan, B. A. Boville, B. P. Breigleb, D.Williamson, and P. Rasch, (1996): Description of the ncar community climate model (ccm3), Tech. Rep. NCAR/TN-420+STR, National Center for Atmospheric Research.
Lejenas, H. and Hansokland, R. (1983), Characteristics of northern hemisphere blocking as determined from a long time series of observational data. Tellus, 35A, 350-362.
Liu, Q. (1994), on the definition and persistence of blocking. Tellus, 46, 286-298.
Liu, Q. (1993), On the definition and persistence of blocking. Tellus, 46A, 286-298.
Liu Q., and Opsteegh T. (1995), Interannual and decadal variations of blocking activity in a quasi-geostrophic model, Tellus 47A, 941-954.
Lupo, A.R., et al., (2007), Assessment of the impact of the planetary scale on the decay of blocking and the use of phase diagrams and enstrophy as a diagnostic. Izv Acad. Sci. USSR, Atmos. Oceanic Phys., 43, 45–51.
Lupo A. R. and Smith P.J. (1994), Climatological features of blocking anticyclones in Northern Hemisphere, Tellus, 47A, 439-456.
Lupo A. R. and Smith P.J. (1994), Planetary and synoptic-scale interactions during the life cycle of a mid-latitude blocking anticyclone over the North Atlantic, Tellus, 47A, 575-596.
Lupo A. R. Clark J. V. Hendin, A. M. Kelly, A. S. Mihalka, K. M. Perrin B. L. Puricelli, K. M. (2008): The global increase in blocking occurrences, CVC, AMS, 19-24.
Lyapunov A.M., (1966), Stability of motion, Academic Press.
Namias J. (1947), characteristics of the general circulation over the northern hemisphere during the abnormal winter 1946-1947. Mon. Wea. Rev., 75, 145-152.
Pal J. S., E. E. Small, and E. A. B. Eltahir, (2000), Simulation of regional-scale water and energy budgets: Representation of subgrid cloud and precipitation processes within RegCM, J. Geophys. Res.-Atmospheres, 105(D24), 29,579–29,594.
Palmen E. and Newten C.,(1969), Atmospheric circulation systems, Academic press, New York London, 335-341.
Patterson J. C., and P. F. Hamblin, (1988), Thermal simulation of a lake with winter ice cover, Limn. Oceanography, 33, 323–338.
Pelly J. L. and Hoskins, B. J. (2002), A new perspective on blocking, Met, dep. Reading United Kingdom, 743-754.
Perkey D. J., and C. W. Kreitzberg, (1976), A time-dependent lateral boundary scheme for limited -area primitive equation models, Mon. Wea. Rev., 104, 744–755.
Rex, D. F. (1950a), Blocking action in the middle troposphere and its effect upon regional climate, (I) An aerological study of blocking action. Tellus, 2, 96-211.
Rex, D. F. (1950b), Blocking action in the middle troposphere and its effect upon regional climate. (II) The climatology of blocking action. Tellus, 2, 275-301.
Rex, D. F. (1951), The effect of Atlantic blocking action upon European climate. Tellus, 3, 100-111.
Shukla J. and Mo K. C., (1983), Seasonal and geographical variation of blocking, Mon. Wea. Rev. 111, 388-402.
Slingo J. M., (1989), A gcm parameterization for the shortwave radiative properties of water clouds, J. Atmos. Sci., 46, 1419–1427.
Smith, P. J. and Tsou, C. H. (1991), Energy transformations associated with the synoptic and planetary scales during the evolution of blocking anticyclone and an upstream explosively-developing cyclone. Tellus, 44A, 252-260.
Sundqvist, H., E. Berge, and J. E. Kristjansson, (1989), The effects of domain choice on summer precipitation simulation and sensitivity in a regional climate model, J. Climate, 11, 2698–2712.
Tibaldi, S. and F. Molteni, (1988): On the operational predictability of blocking. Proceedings of the ECMWF Seminar on The nature and prediction of extratropical weather systems (ECMWF, Reading, U.K., 7-11, Sept. 1987), vol. 2, 329-371. (cf. a11)
Tibaldi, S. and Ji, L. R. (1982), On the effect of model resolution on numerical simulation of blocking. Tellus, 35A, 28-38.
Tibalidi S. and Buzzi A., (1983), Effects of orography on Mediterranean lee cyclogenesis, and its relationship to European blocking, Tellus, 35A, 269-286.
Tibalidi S. and Molteni, (1990), On the operational predictability of blocking. Tellus, 42A, 343-365.
Treidl R. A., Birch F. C. and Sajecki, P., (1981), Blocking actionin the Northern Hemisphere a climatological study.

Tsou, C. H. and Smith, P.J. (1990), The role of synoptic planetary scale interactions during the development of a blocking anticyclone. Tellus, 42, 174-193.
Tsou, C. H. and Smith, P. J. (1998), The important of non-quasigeostrophic forcing during the development of blocking anticyclone. Tellus, 42A, 328-342.
Tung, K. K. and Lindzen, R. S. (1979), A theory of stationary long waves. Part I : A sample theory of blocking. Mon. Wea. Rev., 107, 714-734.
White, W. B. and Clark, N. E. (1975), On the development of blocking ridge activity over the central north Pasific J. Atoms. Sci., 32, 489-501.
Wiin, C. and Wiin, N. (1996), Blocking as a wave-interaction, Tellus, 48, 254- 271.
Y. Y. Hafez, (1997): "Concerning the Role Played by Blocking Highs Persisting Over Europe on Weather in the Eastern Mediterranean and its Adjacent Land Areas". Ph. D. Thesis, Faculty of Science, Cairo University.
Y. Y. Hafez, (1995), Impact Study Concerning the Effect of Blocking Highs Persisting over Eastern Europe on Weather in Egypt". M. Sc. Thesis, Faculty of Science, Cairo University.
Y. Y. Hafez (2007), The Connection between the 500 hpa Geopotential Height Anomalies over Europe and the Abnormal Weather in Eastern Mediterranean during winter 2006. I. J. Meteorology, U. K., Vol., 32, No., 324, 335-348.
Y.Y. Hafez (2008): The Role Played by Blocking over the Northern Hemisphere on Hurricane Katrina. The Journal of American Science, Vol. 4 – No. 2, pp: 10-25.
Y.Y. Hafez (2009): The Role Played By Azores High in Developing of Extratropical Cyclone Klaus. Journal of American Science 2009; 5(5):145-163.
Y.Y. Hafez (2012): Blocking Systems Persist over North Hemisphere and Its Role in Extreme Hot Waves over Russia during summer 2010. Journal of Atmospheric Model Applications, pp, 137-155.
Zeng, X., M. Zhao, and R. E. Dickinson, (1998), Intercomparison of bulk aerodynamic algorithms for the computation of sea surface fluxes using toga coare and tao data, J. Climate, 11, 2628–2644.
Zohdy H. M. (1991): The impact of midlatitudes geopotential anomalies on tropical weather system, PSMP Report series No. 33, WMO publication, pp. 121.